Impact of input FBG reflectivity and forward pump power on RIN transfer in ultralong Raman laser amplifiers

GIUSEPPE RIZZELLI,[1,*] MD ASIF IQBAL,[2] FRANCESCA GALLAZZI,[1] PAWEŁ ROSA,[1] MINGMING TAN,[2] JUAN DIEGO ANIA-CASTAÑÓN,[1] LUKASZ KRZCZANOWICZ,[2] PEDRO CORREDERA,[1] IAN PHILLIPS,[2] WLADEK FORYSIAK[2] AND PAUL HARPER,[2]

[1]Instituto de Óptica "Daza de Valdés", CSIC, Calle de Serrano 121, 28006 Madrid, Spain
[2]Aston Institute of Photonic Technologies, Aston University, Birmingham B4 7ET, UK
*giuseppe.rizzelli@csic.es

Abstract: Relative intensity noise transfer from the pump to the signal in 2nd-order ultra-long Raman laser amplifiers for telecommunications is characterized numerically and experimentally. Our results showcase the need for careful adjustment of the front FBG reflectivity and the relative contribution of forward pump power, and their impact on performance. Finally, our analysis is verified through a 10 x 30 GBaud DP-QPSK transmission experiment, showing a large Q factor penalty associated with the combination of high forward pumping and high reflectivities.

OCIS codes: (060.0060) Fiber optics and optical communications; (060.1660) Coherent communications; (060.2320) Fiber optics amplifiers and oscillators.

References and links

1. J. D. Ania-Castañón, "Quasi-lossless transmission using second-order Raman amplification and FBG," Opt. Express **12**(19), 4372–4377 (2004).
2. P. Rosa, J. D. Ania-Castañón, and P. Harper, "Unrepeatered DPSK transmission over 360 km SMF-28 fibre using URFL based amplification," Opt. Express **22**(8), 9687 (2014).
3. M. Tan, P. Rosa, S. Thai Le, I. D. Phillips, and P. Harper, "Evaluation of 100G DP-QPSK long-haul transmission performance using second order co-pumped Raman laser based amplification," Opt. Express **23**(17), 22181–22189 (2015).
4. M. Tan, P. Rosa, I. Phillips, and P. Harper, "Extended Reach of 116 Gb/s DP-QPSK Transmission using Random DFB Fiber Laser Based Raman Amplification and Bidirectional Second-order Pumping," in Optical Fiber Communication Conference, OSA Technical Digest (online) (Optical Society of America, 2015), paper W4E.1.
5. L. Galdino, M. Tan, D. Lavery, P. Rosa, R., I. D. Phillips, J. D. Ania Castañón, P. Harper, R. I. Killey, B. C. Thomsen, S. Makovejs, and P. Bayvel, "Unrepeatered Nyquist PDM-16QAM transmission over 364km using Raman amplification and multi-channel digital back-propagation," Opt. Lett. 40, 3025-3028 (2015).
6. I. Phillips, M. Tan, M. F. Stephens, M. McCarthy, E. Giacoumidis, S. Sygletos, P. Rosa, S. Fabbri, S. T. Le, T. Kanesan, S. K. Turitsyn, N. J. Doran, P. Harper, and A. D. Ellis, "Exceeding the Nonlinear-Shannon Limit using Raman Laser Based Amplification and Optical Phase Conjugation," in Optical Fiber Communication Conference, OSA Technical Digest (online) (Optical Society of America, 2014), paper M3C.1.
7. P. Rosa, S. Thai Le, G. Rizzelli, M. Tan, and J. D. Ania-Castañón, "Signal power asymmetry optimisation for optical phase conjugation using Raman amplification," Opt. Express **23**(25), 31772–31778 (2015).
8. C. R. S. Fludger, V. Handerek, and R. J. Mears, "Pump to Signal RIN Transfer in Raman Fiber Amplifiers," J. Lightwave Technol. **19**(8), 1140 (2001).
9. B. Bristiel, S. Jiang, P. Gallion, and E. Pincemin, "New model of noise figure and RIN transfer in fiber Raman amplifiers," IEEE Photonics Technology Letters **18**(8), 980–982 (2006).
10. M. Tan, P. Rosa, M. A. Iqbal, I. Phillips, J. Nuño, J. D. Ania-Castanon, and P. harper, "RIN Mitigation in Second-Order Pumped Raman Fibre Laser Based Amplification," in Asia Communications and Photonics Conference 2015, OSA Technical Digest (online) (Optical Society of America, 2015), paper AM2E.6.
11. M. Tan, P. Rosa, S. T. Le, Md. A. Iqbal, I. D. Phillips, and P. Harper, "Transmission performance improvement using random DFB laser based Raman amplification and bidirectional second-order pumping," Opt. Express **24**(3), 2215–2221 (2016).
12. S. B. Papernyi, V. I. Karpov, and W. R. L. Clements, "Third-order cascaded Raman amplification," in Optical Fiber Communications Conference (Optical Society of America, 2002), paper FB4.

13. V. Karalekas, J. D. Ania-Castañón, P. Harper, S. A. Babin, E. V. Podivilov, and S. K. Turitsyn, "Impact of nonlinear spectral broadening in ultra-long Raman fibre lasers," Opt. Express **15**(25), 16690–16695 (2007).

14. M. Alcón-Camas, and J. D. Ania-Castañón, "RIN transfer in 2nd-order distributed amplification with ultralong fiber lasers," Opt. Express **18**(23), 23569–23575 (2010).

15. J. Nuño, M. Alcon-Camas, and J.D. Ania-Castañón, "RIN transfer in random distributed feedback fiber lasers," Opt. Express **20**(24), 27376–27381 (2012).

16. G. Rizzelli , M. A. Iqbal, P. Rosa, M. Tan, L. Krzczanowicz, I. Phillips, W. Forysiak, J. D. Ania-Castañón, and P. Harper, "Impact of Front-FBG Reflectivity in Raman Fiber Laser Based Amplification," in Conference on Lasers and Electro-Optics, OSA Technical Digest (2016) (Optical Society of America, 2016), paper SF1F.6.

1. Introduction

Raman amplification schemes are capable of providing distributed amplification over tens of km as opposed to traditional EDFA based lumped amplification. In these systems, gain distribution allows for a smoother variation of the signal power in transmission and, therefore, for a reduction of amplified spontaneous emission (ASE) noise and a significant improvement of the transmission distance. This is especially true for second- or higher-order (i.e. when pump and signal are two or more Stokes shifts apart), bidirectionally pumped configurations [1] in which an equal amount of pump power should ideally be provided by the forward (FW) and backward (BW) propagating pumps in order to obtain the flattest possible signal power variation (SPV). 2nd-order, ultra-long Raman fiber laser (URFL) amplifiers have consistently proved to be an excellent option in terms of maximum reach for both unrepeatered and long-haul multi-channel coherent transmission systems [2–4] using advanced modulation formats in combination with nonlinearity compensation techniques such as digital back propagation (DBP) or optical phase conjugation (OPC) [5, 6]. However, extended reach comes at the cost of an increase in required pump power and, more importantly, is limited by the relative intensity noise (RIN) transferred from the FW pump to the signal. In fact, assuming that the SPV is sufficiently low and that deterministic fiber nonlinear effects generated during the transmission can be entirely compensated for, the RIN transferred from fiber pump lasers to the signal becomes the most problematic effect when the use of symmetric bidirectional pumping is needed (i.e. in an OPC-based system [7]) or, in wider terms, whenever a certain amount of FW pump power can be beneficial to reduce SPV and improve OSNR [8, 9]. Nevertheless, recent works [10, 11] have shown that random distributed feedback laser (rDFB) amplifiers [12] can be suitable for overcoming RIN impairments enabling transmission distances up to 7915 km for a 10 x 116 Gb/s DP-QPSK long-haul system by removing the fiber Bragg grating (FBG) at the input side of an URFL, thus essentially transforming a Fabry-Perot-like closed cavity into an half-open cavity, at the expense of an additional reduction of the FW pumping efficiency.

Here we present a detailed numerical and experimental investigation of the RIN transfer from the pumps to the signal when the backreflections level (FBG effective reflectivity) at the input side of a 2nd-order Raman amplifier is varied from 0% (half-open cavity rDFB) to 95% (high-efficiency URFL) and the FW pump power is gradually increased from 0% (BW only pumping) to 100% (FW only pumping) of the total pump power. To do so we characterize various configurations in terms of output signal RIN and mode structure of the first Stokes component at 1455 nm. Moreover, we present the transmission performance of a WDM 10 x 30 GBaud DP-QPSK coherent transmission system, showing the Q factor as a function of the propagation distance when different cavity configurations are used as the core building block of a recirculating loop for emulating long-haul communication.

2. Experimental setup

The schematic diagram of the 2nd-order Raman laser amplifier is shown in Fig. 1. Two fully depolarized, virtually identical fiber lasers emitting at 1366 nm bidirectionally pump 100 km of standard ITU G.652 single mode fiber.
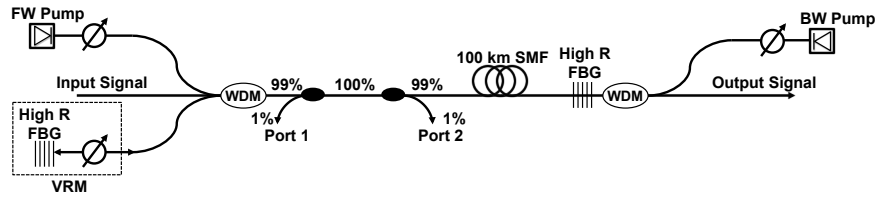
Fig. 1. Experimental setup of a 2nd-order Raman laser amplifier with variable input-side reflectivity.

A wavelength division multiplexer (WDM) is used at each end of the fiber to couple/split three signals: the pump, the generated first Stokes component at the 1455 nm central wavelength of the high reflectivity FBG at the output side and an injected -10 dBm CW signal at 1550 nm. The 1455 nm port of the WDM at the input is connected to a variable reflectivity module (VRM) that provides an adjustable amount of backreflections. The VRM is composed of a variable optical attenuator (VOA) and a high reflectivity (>95%) FBG centered at 1455 nm. The VRM can reflect up to 40% of the incident light back into the cavity. The VRM effective reflectivity, which is limited by the losses of connectors and the WDM itself, is constantly monitored by means of two 99/1 splitters used to tap out part of the incident and reflected Stokes wave. Lastly, two VOAs placed at the output of both pump lasers are used to regulate the injected FW and BW pump powers while maintaining their output power and, therefore, keeping the output RIN fixed. By avoiding direct manipulation of the pump lasers' current we ensure that signal RIN is exclusively affected by the combined effect of the reflectivity and pump power ratio.
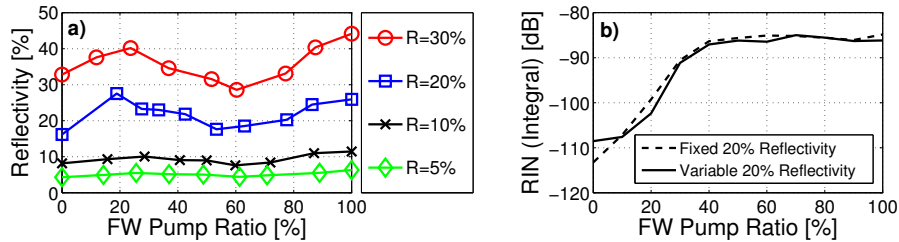

Fig. 2. (a) Input-side reflectivity vs. FW pump ratio and (b) signal RIN integrated over 1MHz for a 20% variable (solid) and fixed (dashed) input FBG reflectivity.

Another possible uncertainty factor that can have an impact on RIN transfer to the signal is the variation of the FBG central wavelength with the incident power [13]. An increase in the pump power incident on the FBG causes spectral broadening of the 1455 nm lasing and a deviation of the central wavelength from the nominal value due to thermal expansion. Fig. 2(a) shows the reflectivity provided by the VRM as a function of the FW pump ratio (FPR) for four different attenuation settings of the VOA inside the VRM, corresponding to 5%, 10%, 20% and 30% reflectivity. Effective reflectivity was measured as the ratio of the reflected power at port 2 to the incident power at port 1, whereas the FW pump ratio is the percentage of total pump power provided by the FW pump. Total pump power is adjusted to obtain zero net gain for the signal at the amplifier output. As expected the reflectivity excursion is greater when the VOA attenuation is lower, as more light is let through to the FBG, but all of the four curves exhibit the same trend with a local maximum at about 20% FW pump power ratio, a minimum around 60% where the first Stokes power is highest, and an absolute maximum at 100% when the total pump power injected into the cavity is lowest. However, large excursions of over 10% when the initial reflectivity value is set to 20% or 30% do not have any impact on the measured signal RIN. RIN was measured using a low noise photodetector with a 125MHz bandwidth and integrated over the first 1 MHz. The VRM VOA attenuation was adjusted to obtain 20% reflectivity for BW only

pumping and then, following two different approaches, kept fixed, as the FW pump ratio was increased, in order to produce the variable reflectivity shown in Fig. 2(a) or carefully adjusted to achieve full compensation of the backreflections variation. The comparison shown in Fig. 2(b) presents no appreciable difference: RIN evolves nearly identically in both cases according to the typical S-shaped trend.

3. Cavity characterization

As indicated above, fiber pump lasers exhibit a RIN level dependent on their drive current. Fig. 3 shows how the output signal RIN varies when the RIN of the pumps is allowed to vary with the pump power, as opposed to the adopted fixed RIN solution accomplished through external attenuation of the pumps' output powers. The integrated RIN is presented as a function of the FPR for cavity configurations with the highest (40%) and the lowest (1.5%) achievable backreflections. The latter was obtained by replacing the VRM with a straight FC/PC connector.
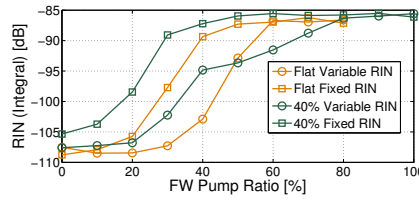

Fig. 3. Signal RIN integrated over 1MHz for variable (solid) and fixed (dashed) pump RIN in the 1.5% and 40% reflectivity cases.

The RIN level is comparable in all four cavity designs when only the BW pump is used to amplify the signal to the initial power. As the FW pump power contribution is increased, the pump-to-signal RIN transfer functions follow a dissimilar growth. The cavity most resilient to the effect of the FW pump is the one with the lowest input-side reflections and variable RIN. A FPR as high as 30% is admissible in this case with negligible penalty in terms of output signal RIN. On the other hand, feeding a fixed amount of pump RIN into the same cavity results in 10 dB integrated RIN penalty for the same 30% FPR. Furthermore, if we consider -100 dB as a reference point on the rising slope of the integrated RIN curves, the effect of the reflectivity on the maximum admissible FW pump ratio becomes clear. Regardless of the pump RIN being variable or fixed, the reduction in FPR amounts to about 10% when the input-side reflectivity is increased from 1.5% to 40%.

As our intention is to analyze the joint effect of reflectivity and FW pump power on RIN transfer, hereafter the pumps RIN levels are considered fixed unless otherwise stated.

Fig. 4 shows the Stokes lasing component mode structure measured in FW and BW direction for FPR up to 50%. It can be noticed that for a half-open cavity with no reflections at the input side (rDFB) the 1455 nm wave does not present any sign of structure thus confirming the dominance of random lasing with Rayleigh backscattering feedback in both directions. The lack of a seeded forward Stokes component is also visible in the low-reflectivity (1.5%) cavity and in the high-reflectivity (40%) one with a fundamental difference: beyond a certain limit of the FW pump ratio these two partially-closed cavities do show fairly well defined modes, as cavity lasing begins to dominate. In the 1.5% reflectivity configuration the FPR threshold is 30% both in the FW and BW direction, whereas in the 40% reflectivity cavity it is 10% and 20% in the FW and BW direction respectively.

These values reflect remarkably well the evolution depicted in Fig. 3 and confirm that it is the presence of the FW-propagating 1455 nm seed that mediates in the RIN transfer between the high-order pump and the signal. As a result, 1.5% reflectivity allows for a 20% FPR, with low-RIN operation whereas, with a 20% FPR, a high reflectivity in the order of 40%, causes the RIN to get more easily transferred and leads to a 7 dB RIN penalty.
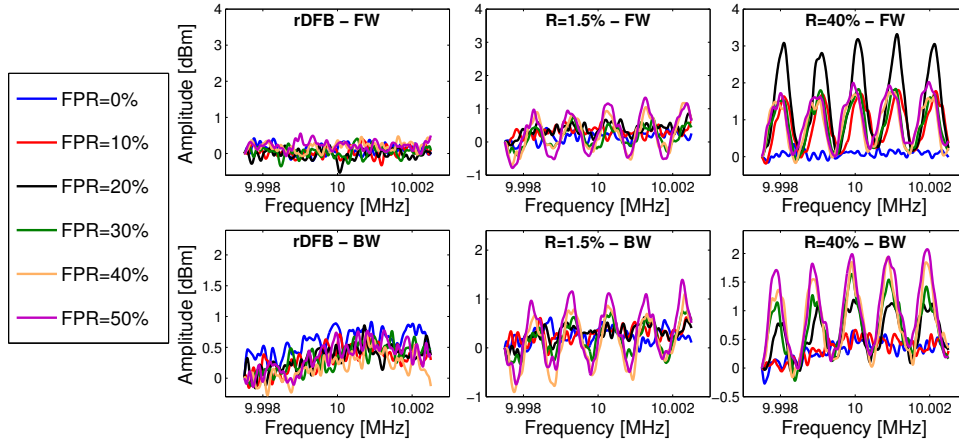
Fig. 4. FW (upper row) and BW (lower row) propagating Stokes mode structure for rDFB, 1.5% reflectivity and 40% reflectivity configurations.

A more comprehensive cavity characterization for different reflectivity values is presented in Fig. 5(a). All of the cavities, including the half-open rDFB, suffer from higher RIN transfer with increasing FW pump power. The higher the front-end reflectivity, the lower the FW pump power can be before the signal RIN starts to increase and the steeper the integrated signal RIN growth is. Interestingly, RIN transfer seems to saturate for FW pump ratios above 50%, so further increasing FW pump power does not greatly affect performance.
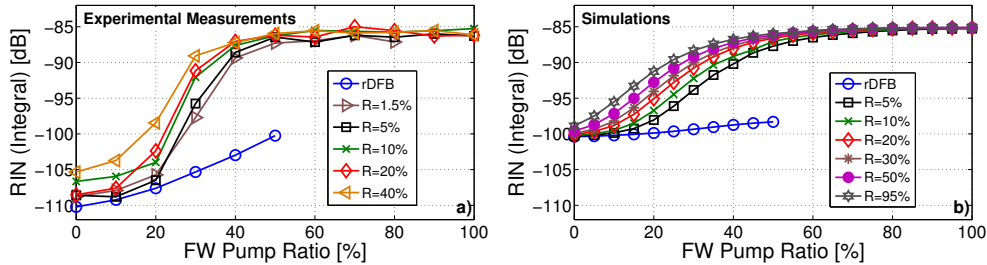

Fig. 5. (a) Experimental and (b) simulated signal RIN integrated over 1MHz as a function of the pump power split and front-end reflectivity for a 100 km 2nd-order ultra-long Raman laser amplifier.

Numerical simulations following the model presented in [14, 15] were used to investigate this behavior for FW pump ratios above 40%. The results, including the effects of depletion, attenuation, Rayleigh backscattering, ASE and using the actual measured output RIN of the pump lasers, are presented in Fig. 5(b). These show good agreement with experimental RIN trends, with the minor differences in absolute values attributable to small deviations from the stock fiber characteristics used in the simulation.

4. Transmission results

In recent work [16] we have shown that the use of a rDFB in a 2000 km long single channel DP-QPSK coherent transmission system, with variable RIN conditions, allows for RIN-free communications for FPR up to 40%, whereas a 10% front reflectivity combined with 40% FPR results in over 1 dB Q factor penalty. Here, in order to quantify the extent to which the RIN transferred to the signal affects the transmission performance in a WDM system we present

experimental results for a 10 x 30 GBaud coherent detection DP-QPSK system. The variable input-reflectivity 2nd-order Raman fiber amplifier shown in Fig. 1 was used for the Raman amplified span in the recirculating loop outlined in [4]. Q factor (converted from bit error rate) was measured while varying the signal launch power into the span at different backreflection levels.
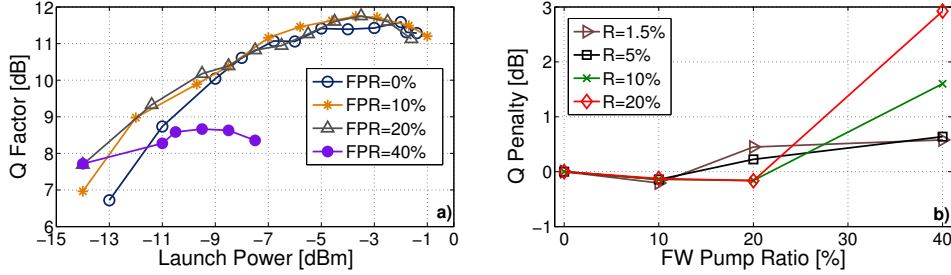

Fig. 6. (a) Q factor vs launch power for a 20% front reflectivity cavity and (b) Q penalty as a function of the FPR for four different cavities in a 2159 km long 10 x 30 GBaud DP-QPSK coherent transmission system.

Fig. 6(a) shows how the Q factor evolves with the launch power of the middle WDM channel channel at 194 THz for an illustrative reflectivity of 20% and FW pump ratios ranging from 0% to 40%. The optimal launch power is approximately -4 dBm for up to 20% FPR and reduces to approximately -9.5dBm for 40% FPR. The Q penalty due to the FW pump power is self-evident and it becomes clear by looking at Fig. 6(b) where it is plotted against the FPR for different reflectivity levels. The launch power per single channel is the optimal for each cavity configuration and the transmission distance is 2159 km. Cavities with front-reflectivity below 5% can tolerate pump ratios up to 40% paying a penalty of about 0.6 dB to the BW only pumping configuration. Backreflections of 10% and 20% lead to a non-negligible drop in the Q factor by 1.6 and 2.9 dB respectively for a 40% FPR.

5.   Conclusion

We have presented an in-depth characterization of an ultra-long 2nd-order Raman fiber amplifier with variable front-end reflectivity showing, experimentally and numerically, how the RIN transferred from the high order pump at 1366 nm to the signal at 1550 nm evolves with the FW pump ratio when the reflectivity at the input side of the cavity is gradually increased. We have isolated the joint effect of FW pump and front-end reflectivity by adjusting the pump power ratios through attenuation of fixed output powers and shown a 10% reduction in the maximum acceptable forward pump ratio with respect to variable pumps RIN conditions. The 1455 nm Stokes component's role in the RIN transfer has been analyzed through measurement of the laser mode structure, confirming the relevance of the threshold between a random, low-RIN transfer lasing regime and a cavity-lasing seeded one. Finally, we have evaluated the test-bed performance of a WDM 10 x 30 GBaud DP-QPSK coherent transmission system based on different cavity architectures. Our measurements show that the combination of input-side reflectivity and forward pump power needs to be carefully considered. With a high forward pump ratio (above 20%) a significant Q penalty can be avoided by using a low reflectivity value, which also enables over 20% higher pumping efficiency with respect to a perfect rDFB.

Funding